Cement and Concrete Research 42 (2012) 549–557

Contents lists available at SciVerse ScienceDirect

Cement and Concrete Research

journal homepage: http://ees.elsevier.com/CEMCON/default.asp

Relationship between inter-aggregate spacing and the optimum fiber length for spalling protection of concrete in fire

Young-Sun Heo [a], Jay G. Sanjayan [b,*], Cheon-Goo Han [c], Min-Cheol Han [c]

[a] Department of Civil Engineering, Monash University, Clayton, Victoria 3800, Australia
[b] Engineering and Industrial Sciences, Swinburne University of Technology, PO Box 218, Hawthorn, Victoria 3122, Australia
[c] Department of Architectural Engineering, Cheongju University, Cheongju, Chungbuk, Republic of Korea

ARTICLE INFO

Article history:
Received 1 April 2011
Accepted 6 December 2011

Keywords:
A. Temperature
B. Interfacial transition zone
E. Fiber reinforcement
E. Concrete
Fire

ABSTRACT

Addition of polypropylene fibers in concrete for spalling protection in fire is well known, where the fibers melt in fire and percolate the concrete. However, the optimum fiber characteristics for spalling protection are not well understood. In this study, the optimum fiber length for spalling protection of concrete is found to be related to the inter-aggregate spacing of coarse aggregates, which is critical for the interconnectivity of adjacent aggregates surrounded by porous interfacial transition zones. The experimental test results showed that, for the concrete with maximum 20 mm of graded aggregates, with optimum 30 mm length fibers, almost no spalling was found; whereas other fiber concretes lost up to 92% of weight due to spalling. By evaluating the criteria of the optimum fiber length, this study also found the critical threshold of fiber numbers per unit volume.

1. Introduction

High strength concrete as a construction material has many advantages, and, in recent years, it has become popular due not only to its high strength but also due to its high durable performance, especially for infrastructure including tunnels and high rise buildings. In a fire event, however, high strength concrete performs very poorly by comparison to normal strength concrete [1–3]. Although there are a number of ways to mitigate the risk of spalling in high strength concrete, it is necessary to quantify other criteria, in order to achieve the optimum level of spalling protection, in which polypropylene fiber addition as an effective measure is chosen in this study.

The spalling mechanism for high strength concrete is not fully understood, but possible explanations can be made using either thermo-mechanical theory [4,5], moisture clog theory [6–8], or a combination of both theories [9,10]. According to the thermo-mechanical theory, spalling occurs due to the fact that a thermal gradient and thermal incompatibility lead to high stresses close to the surface of concrete being exposed to fire. High strength concrete with high brittleness cannot tolerate these two stresses and consequently causes the failure of the concrete during fire, whereas normal strength concrete with relatively low brittleness seems to accommodate the induced stresses. According to the moisture clog theory, on the other hand, it is important to understand the flow of water vapor and its pathways, which is likely to be impeded by the low permeability system in high strength concrete. This theory is more widely accepted in the literature as compared with the thermo-mechanical theory. A percolation theory gives detailed information that describes the pathways for the water vapor in cement-based materials at a microscopic level. Brief introduction of the moisture clog and the percolation theories are described below.

Concrete contains substantial amount of water in the form of free liquid water and physically/chemically bound water, which is dependent on a water to cement ratio, a curing condition and other environmental factors after the curing. According to Avogadro's law and Charles's law, if the density of water is regarded as 1 g/cm^3, 1 cm^3 (= 1 g) of water at 20 °C will expand to 1579 cm^3 of gas at 100 °C. Such an expansion increases the pore pressure in high strength concrete in fire. The moisture clog theory indicates that, in a fire event, the water vapor in concrete migrates deeper into concrete in which the pressure is lower and temperature is cooler, which might cause the condensation of the vapor. The dense pore structure in high strength concrete interferes with the return of the condensed vapor outside concrete. As the vaporize–migrate–condense cycle continues, accumulation of vapor will build up in the cooler regions until finally a completely saturated layer (moisture clog) is formed [6]. Once the moisture clogs are created, they make the flow of the vapor more difficult and accelerate the increase of pore pressure, thus resulting in the failure of lateral forces of the concrete. Percolation theory [11–13] deals with the connectivity of components in a system. In particular, Bentz [11] has reported that big porous zones of normal strength concrete can be obtained by thick interfacial transition zones (ITZs), in which percolation from top to bottom can be achieved. Bentz [11] proposed that if the capillary porosity in the individual ITZs remains

* Corresponding author. Tel.: +61 3 92148034; fax: +61 3 92148364.
E-mail address: jsanjayan@swin.edu.au (J.G. Sanjayan).

0008-8846/$ – see front matter © 2011 Elsevier Ltd. All rights reserved.
doi:10.1016/j.cemconres.2011.12.002

percolated and the ITZs themselves are percolated, a convenient escape route for the vapor generated during fire exposure may exit. It should be noted that the level of concrete permeability is governed by the porosities of ITZs. The breakdown of the ITZs reduces the solidity of the concrete and the opening channels [14]. Scrivener [15] proposed that the inclusion of aggregate disrupts the packing of cement particles locally resulting in a high water to cement ratio in this ITZs. Scrivener and Nemati [13] also suggested that the ITZ regions (estimated thickness of conventional concrete: 20 μm) are percolated.

Hence, for high strength concrete that is not percolated due to relatively thinner ITZs as compared with normal strength concrete, the isolated porous ITZs region can be connected by the addition of synthetic fibers with low melting point, such as polypropylene fibers [8,16–19], so that the vapor can evacuate through the connected porous network. Regarding the effectiveness of fibers for spalling protection, some researchers [20,21] have agreed that longer length of fibers is more efficient than shorter length of fibers. This is due to the fact that the main role of fiber addition is to provide the link between the isolated ITZs, and thereby long fibers are beneficial to bridge the isolated porous regions located further apart. In previous work conducted by the authors [22–24], however, conflicting result has been consistently observed as follows.

Fiber length is in some cases critical for spalling protection of concrete, but in other cases the total number of fibers is critical. For a given fiber content, V_f, both the fiber length, L_f, and fiber diameter, d_f, affect the total number of fibers per unit volume, N. The relationship is given by

$$N = \frac{4V_f}{\pi d_f^2 L_f}. \tag{1}$$

It has been found that, for a given type of fibers, if the combination of N and L_f, NL_f^3, is used as the measure for the fiber addition, the constant predictable results for the degree of concrete spalling was obtained, regardless of fiber contents. Decreasing the L_f increases N, so that fibers with shorter length can have higher value of NL_f^3 (mostly with fine diameter fibers), compared to fibers with longer length [24]. However, a critical fiber length to optimize the performance of spalling protection is unknown.

For further research, thus, it is crucial to find the optimum length of fibers, satisfying the level of interconnectivity (related to the function of L_f) and securing a well distributed network (related to the function of N) for the pressure relief of vapor produced in fire. Since the thickness of ITZs is much smaller than the distance of two adjacent aggregates, and the required threshold length of fibers to connect these regions does not need greater accuracy than ± 10 μm. This distance hereafter is referred to as inter-aggregate spacing for convenient calculations.

However, the inter-aggregate spacing is mainly determined by the size of the aggregates, and the data reporting this effect on the spalling of concrete are practically limited. It is hypothesized that the dominant factor of fiber parameters (either long L_f with small N or short L_f with large N) to resist concrete spalling is dependent on this criterion of the aggregate, due to the fact that the inter-aggregate spacing is a key parameter to determine the least fiber length for the concrete to be percolated. Therefore, by analysing the relationship of the size of the aggregate and the fiber parameters, this study aims to provide quantitative information, which can offer an approach to predict the optimum length of fibers for any concrete of a given aggregate size and grading.

2. Theoretical background

2.1. Specific surface area of aggregates

Total specific surface area of aggregates gives information about the characteristics of various sized and graded aggregates, and it is an essential parameter for calculating the inter-aggregate spacing. In this study, all calculations were made based on the assumption that all aggregates were spherical.

There are a number of ways to estimate the specific surface area of the aggregates. For a single aggregate, simple geometric estimation has been proposed by Chapuis et al. [25] as follows:

$$S_s = \frac{6}{d_a \rho_S}. \tag{2}$$

where S_s is the specific surface area (in m^2/kg) of the single aggregate, d_a is the diameter of the aggregate and ρ_s is the density (kg/m^3) of the aggregate. For graded aggregates, Loundon [26] calculated it based on a sieve analysis with the assumption that all aggregates were uniformly distributed in the size between the mesh size (mm) d_x and d_y of adjacent sieves as given by

$$S_i = \frac{6}{\sqrt{d_x d_y}}. \tag{3}$$

where S_i is the specific surface area (in m^2/L) of the graded aggregates. Starting with Eq. (3), this study introduces void space volume, η (from Eq. (6)), of dry rodded aggregate and density, ρ_s, which is equal to the aggregate used in this study, in order to obtain the specific surface area of the aggregate in m^2/kg. This is given by

$$S = \frac{6}{(1-\eta)\rho_S \sqrt{d_x d_y}} \tag{4}$$

This calculated specific surface area by Eq. (4) is used as an indicator to calculate the actual specific surface area, S_{tm}, of the used aggregate having fractions of the total mass retained on different sieves. This is given by

$$S_{tm} = \sum_{x=1}^{n} S_x \chi_x \tag{5}$$

where $S_1\ S_2 \cdots$ and S_n is the specific surfaces of uniform spheres distributed in the different sieves, and $x_1\ x_2 \cdots$ and x_n is the total mass of the actual used aggregate retained on the corresponding sieves. The calculated S_{tm} are shown latter in Table 4.

2.2. Inter-aggregate spacing

The inter-aggregate spacing is calculated based on a shell model suggested by Rangaraju [27]. In this shell model, however, the exclusive inter-aggregate spacing of coarse aggregate was not considered on purpose, due to the fact that the sand fraction exhibits much greater area in contact with cement paste than does the coarse aggregate.

However, in the aspect of vapor evacuation in fiber added concrete in a fire event, the level of pore connectivity is more important than the level of pore's specific surface area. Although the total specific surface area of fine aggregate associated with ITZs is high, it is obvious that the circumference of the each ITZ surrounding a sand grain in fine aggregate concrete is short and isolated, whereas the ITZ in coarse aggregate is long and thereby connected. Neithalath [28] uses morphological measures to characterize the pore connectivity. In this research, it has been found that maximization of water transport behavior is best achieved by increasing the pore connectivity factor, and the use of large sized aggregate is definitely a viable means of increasing the pore connectivity. According to the simulation by Bentz [11] for the concrete at elevated temperature, it has been observed that it is mainly the larger aggregates that are a part of the percolated pathway, and not the smaller aggregates that provide a major fraction of the aggregate surface area. Hence, a modified shell model, C_{shell} model, is proposed in the present study to take account this effect of the inter-aggregate spacing of coarse aggregates ($\acute{\iota}$).

In the C_{shell} model, (1) void space volume, **η**, of dry rodded aggregate possessed by the total amounts of the coarse aggregates used in the present study, (2) the excess volume of mortar, **ε**, after filling '**η**' and (3) the thickness of the mortar shell covering each coarse aggregates by '**ε**' are calculated. Finally, (4) the inter-aggregate spacing of the coarse aggregates, *ί*, is twice the mortar shell thickness as can be seen latter in Fig. 9. This is based on the assumption that all of the coarse aggregates are enveloped by a shell of mortar of uniform thickness, in which a conceptual idea is again similar to the shell model by Rangaraju [27]. Detailed calculation is presented as follows.

For (1) **η**, it is given by

$$\eta = \gamma - \left(\frac{\omega}{\rho_S}\right) \tag{6}$$

where γ is the total volume (**η** + aggregate volume) of dry rodded aggregate possessed by the amounts of the coarse aggregates used in the present study, which is determined as the total amounts of the coarse aggregates, ω, divided by dry rodded unit weight, A_w, of the coarse aggregate; and ρ_s is the density of the coarse aggregates. For (2) **ε**, it is given

$$\varepsilon = V_{conc} - \gamma \tag{7}$$

where V_{conc} is the total volume of the concrete. For (3) the thickness of the mortar shell, it is calculated by dividing **ε** (Eq. (7)) by the total surface area of the coarse aggregates, which is determined as S_{tm} (Eq. (5)) multiplied by ω. For (4) *ί*, it is given by

$$i = 2\left(\frac{\varepsilon}{S_{tm}\omega}\right) \tag{8}$$

The calculated *ί* used in this study and their required parameters are shown latter in Table 5.

3. Experimental work

3.1. Experimental outline

Table 1 shows the experimental outline of this study. Various combinations of fiber length (6, 9, 12, 19, 30 and 40 mm) and maximum aggregate size (4, 10, 20 and 32 mm) were added in concrete and tested for investigating the effect of a correlating work on the spalling protection of the concrete, consequently in order to propose the optimum fiber length. An effect of a fiber diameter (40 and 20 μm) was also investigated for the representative concrete containing maximum 10 mm aggregate. Relatively small fiber content, 0.05% by volume, was chosen in all concretes to distinctively assess the effectiveness of the dimensional fiber characteristics. For a convenient purpose, the specimen with maximum 4 mm aggregate is hereafter also called concrete, and all calculation related to the use of coarse aggregate in this paper is instead carried out with the use of fine aggregate for 4 mm aggregate concrete.

For the test methods conducted in this study (Table 1), slump flow was performed in accordance with ASTM C 1611. Air content was measured according to ASTM C 138. ASTM C 39 was conducted for compressive strength test of hardened concretes. Fire tests were carried out for 1 h according to the standard heating curve of ISO-834. After the test completed, extent of spalling was visually observed, and the weight loss and residual compressive strength of concretes were tested by comparing the values before and after the test. Cylinders of size Ø100 × 200 mm were prepared and tested in triplicate for each type.

3.2. Materials

Ordinary Portland cement (density: 3150 kg/m^3 and fineness: 330 m^2/kg) was used in this study. Fly ash (density: 2210 kg/m^3, fineness: 406 m^2/kg and loss on ignition: 3.5%) and silica fume (density: 2200 kg/m^3, fineness: 20,000 m^2/kg and loss on ignition: 1.5%) were incorporated as mineral admixtures. For aggregates (granite type), the combination of river sand and crushed rock (4:6) was mixed to obtain a 2.6 fineness modulus of fine aggregate. Density and absorption of the both fine aggregates were 2600 kg/m^3 and 0.46%. All coarse aggregates used in this study were a crushed aggregate type. Density and absorption of the coarse aggregates were 2610 kg/m^3 and 0.58%. The concrete mixture proportion and properties of control concrete before and after fire tests are summarized in Table 2. The physical properties of polypropylene fibers are in Table 3.

Table 4 shows the calculated specific surface area of the coarse aggregates based on a sieve analysis. For 4 mm, 10 mm, 20 mm and 32 mm concrete, the corresponding values were 5.54 m^2/kg, 0.41 m^2/kg, 0.30 m^2/kg and 0.21 m^2/kg respectively. Table 5 shows the results of calculated inter-aggregate spacing of the coarse aggregates, *ί*. For 4 mm, 10 mm, 20 mm and 32 mm concrete, the corresponding *ί* were 0.03 mm, 2.65 mm, 3.72 mm and 5.42 mm.

4. Test results

4.1. Properties of the concrete

Fig. 1 shows the slump flow of the concretes. Although the fiber content used in this study was very small (0.05% by volume), the effect of fiber length on concrete workability was significant. Increasing the length of fibers constantly decreased the workability, in spite of the fact that, for a given fiber content, longer fibers had a smaller number of fibers per unit volume than shorter fibers (Eq. (1)). Hence, it can be concluded that the workability of concrete containing fibers is more influenced by the fiber length, rather than the number of fibers per unit volume. This is probably because short fibers have better dispersion than long fibers. In addition, the maximum size of aggregate also had an impact on the concrete workability. This study observed that concrete with 20 mm aggregate had the best results followed by the concretes with 32, 10 and 4 mm aggregate.

Fig. 2 shows the air content of the concretes. In general, the longer the fiber length the greater is the air content. Nevertheless, the air contents of most concretes ranged between 2.5 and 3.5%, except for the 4 mm aggregate concrete where the air contents ranged between 6.0 and 7.5%, which was due to the absence of coarse aggregate.

Fig. 3 shows the compressive strength of the concrete specimens at 28 days. The test results showed that the fiber length was not a contributing factor to the compressive strength of the concretes. The strengths were between 74 and 80 MPa. However, the size of the aggregate had an influence on the strength. Overall, the highest strength was observed in the concretes with 10 mm aggregate, and

Table 1
Experimental outline.

Fiber				Aggregate size (mm)	Test conducted	
Type	Diameter (mm)	Length (mm)	Content (% by volume)		Fresh and hardened concrete	Fire test
Control mix	(No fiber addition)			20	Slump flow	Spalling extent
Polypropylene	0.04	6, 9, 12, 19, 30, 40	0.05	4, 10[a], 20, 32	Air content	Weight loss
					Compressive strength	Residual compressive strength

[a] Also applied to 20 μm diameter fibers with the same various lengths and examined fire tests only.

Table 2
Mixture proportion and properties of control concrete.

W/B[a]	Unit water (kg/m^3)	S/a[b] (%)	Weight mixture (kg/m^3)					Slump flow (mm)	Air content (%)	Compressive strength (MPa)	Weight loss (%)	Residual compressive strength (%)
			C[c]	FA[d]	SF[e]	S[f]	G[g]					
0.25	160	45	448	128	64	665	816	685	3.4	80	92	0

[a] Water to binder ratio.
[b] Sand to aggregate ratio.
[c] Cement.
[d] fly ash.
[e] Silica fume.
[f] Sand.
[g] Gravel.

the next highest was in the concretes with 20 mm aggregate. The concretes with 4 and 32 mm aggregate had up to 10 MPa less than those concretes with 10 and 20 mm aggregates. However, it is important to note that all measured strengths of the concretes in this study place the concretes at high risk of spalling in fire [1–3].

4.2. Extent of spalling

Fig. 4 shows images of the spalling in concretes containing polypropylene fibers with various lengths and aggregates with various sizes. For the control concrete, the detailed properties after fire exposure are shown in Table 2. As expected, weight loss due to spalling was 92%, and residual compressive strength was 0%. The results showed that severe spalling occurred.

For other concretes (Fig. 4), it was visually confirmed that the length of fibers and size of aggregates had an effect on the spalling protection of the concretes. It was very clear that the addition of short fibers with 6 and 9 mm length did not provide any protection from spalling for any of the concrete specimens, regardless of the aggregate size. By contrast, the results of the concretes containing long fibers were inconsistent, thus requiring further explanation. For example, for the addition of 12 mm length of fibers, the spalling resistance was improved for the concretes with 4, 10 and 20 mm aggregates, but was not improved at all for the concrete with 32 mm aggregate. On the other hand, for the addition of 30 and 40 mm fiber lengths, the level of the spalling resistance was significantly improved for the concretes with 20 and 32 mm aggregates, but was very poor for the concretes with 4 and 10 mm aggregates.

In order to explain these inconsistent spalling behaviors that have not been reported in the literature, this paper has introduced a new aggregate parameter, inter-aggregate spacing $\acute{\imath}$ as defined in Section 2.2. As calculated in Table 5, $\acute{\imath}$ is larger for the larger aggregate concretes, compared to smaller aggregate concretes, and in any concretes, fibers longer than the length required to connect the ITZ regions are not helpful. In fact, the presence of such long fibers makes the performance of the fibers for spalling protection deteriorate, because increasing L_f always decreases N for a given fiber content (Eq. (1)). In some cases, the effect of N on spalling protection can overtake the effect of L_f. This crucial effect of the N is shown in the experimental results in Fig. 5.

Fig. 5 shows the extent of spalling in the concretes containing fibers with two different diameters, 40 and 20 μm. It is clear that the optimum length of fibers decreased from between 12 and 19 mm for the concretes containing 40 μm fibers to between 9 and 12 mm for the concretes containing 20 μm fibers. This reduction of the optimum fiber length is due to the increased N. Halving the fiber diameter results in four times higher N (Eq. (1)). Hence, if N is increased by reducing L_f in the fine fiber concrete, the amount of increment is much greater than that in coarse fiber concrete, and thereby this great increase of N in the fine fiber concrete might offset the possible deficiency of the interconnectivity arising from the decreased L_f. This is because the influence of reducing fiber diameter without indirect effect of increasing N is negligible on the relief of vapor pressure due to the fact that water vapor is much smaller than the fiber diameter. Further discussion is made in a statistical manner in Section 5 proposing the threshold of the boundary (critical N) where the effect of N starts to overtake the effect of L_f.

It is important to note that although N of the fibres with 6 mm length added to the concretes was the highest for a given fiber content, the addition of the fibres was not effective even for 4 mm aggregate concrete (Fig. 4), in which the $\acute{\imath}$ was only 0.03 mm (Table 5). In fact, as can be seen in Fig. 4, the addition of the fibres with 12 mm length was the most effective for this 4 mm aggregate concrete. This unexpected finding could be because the ITZs in fine aggregate concrete are mostly isolated and circumferences of the ITZs are small as compared with those of ITZs in coarse aggregate concrete, thus making it unlikely that there will be enough fibres to connect all the sand grains to achieve percolation of the concretes. On the other hand, the finding could be explained by the fact that only those fibers in contact with the exterior surface of the concrete can provide pathways for water vapor flowing out of the concrete during fire [11], and it is assumed that fibres with 6 mm length do not have many fibres to contact with the exterior surface of the concrete. Hence, for 4 mm aggregate concrete, the least length of fibers for the percolation is not influenced by the inter-aggregate spacing of fine aggregate parameter: instead, the length of fibers should be long enough to connect other highly porous regions and to contact the exterior surface of the concrete, which was determined to be 12 mm in this study.

Table 3
Physical properties of polypropylene fibers.

Diameter, mm	Length, mm	Density, kg/m^3	Tensile strength, MPa	Melting point, °C
0.02, 0.04	6, 9, 12, 19, 30, 40	910	560	160

Table 4
Calculated specific surface area of coarse aggregates based on a sieve analysis.

Sieve size, mm	Specific surfaces of uniform spheres of this size (S), m^2/kg (Eq. (4))				Percentage of total retained in this sieve size			
	Max. 4 mm	Max. 10 mm	Max. 20 mm	Max. 32 mm	Max. 4 mm	Max. 10 mm	Max. 20 mm	Max. 32 mm
37.5–26.5	0.10	0.09	0.09	0.09	0	0	0	5
26.5–19.0	0.14	0.13	0.12	0.13	0	0	5.00	35.00
19.0–13.2	0.20	0.18	0.18	0.18	0	0	32.00	25.00
13.2–9.5	0.28	0.25	0.25	0.25	0	10.00	15.00	20.00
9.5–4.75	0.46	0.43	0.42	0.42	3.20	90.00	48.00	15.00
4.75–2.36	0.93	0.85	0.84	0.84	13.40	0	0	0
2.36–1.18	1.86	1.71	1.68	1.68	6.60	0	0	0
1.18–0.6	3.68	3.39	3.33	3.34	28.80	0	0	0
0.6–0.3	7.30	6.73	6.60	6.62	24.20	0	0	0
0.3–0.15	14.61	13.46	13.20	13.24	16.80	0	0	0
Specific surface area of aggregates used (S_{tm}), m^2/kg (Eq. (5))					5.54	0.41	0.30	0.21

Note: For 4 mm aggregate concrete, S_{tm} is the specific surface area of fine aggregates.

Table 5
Inter-aggregate spacing, ℓ, and required parameters, calculated for $V_{conc} = 1\ m^3$.

Max. size of aggregate (mm)	ω, kg	Dry rodded unit weight of coarse aggregates (A_w), kg/m^3	γ (ω/ A_w), m^3	Total specific surface area of coarse aggregates (S_{tm}ω), m^2/kg	ε (Eq. (7)), m^3	ℓ (Eq. (8)), mm
4	1481	1795	0.82	8210	0.12	0.03
10	816	1608	0.51	333	0.44	2.65
20	816	1659	0.49	245	0.46	3.72
32	816	1652	0.49	168	0.45	5.42

Note: V_{conc} includes 4.5% by volume of air content, and all calculations for the concretes with maximum 4 mm aggregate are made with fine aggregate, and thus the calculated values are related to the properties of fine aggregate concrete, i.e. 'ε' is the excess volume of paste as otherwise 'ε' for other concretes is the excess volume of mortar.

4.3. Weight loss due to fire exposure

Fig. 6 shows the weight loss of the concretes containing fibers with various lengths and aggregates with various maximum sizes. It can be clearly seen that each concrete having the aggregates with various maximum sizes had different critical thresholds of the optimum fiber length for minimizing the weight loss due to spalling. This is re-plotted in Fig. 7 showing the optimum fiber length of each concrete against the aggregate sizes used. Increasing the aggregate size proportionally increased the optimum fiber length for spalling protection: for the concretes with 4 mm, 10 mm, 20 mm and 32 mm aggregates, the optimum fiber lengths were 12 mm, 19 mm, 30 mm and 40 mm lengths respectively, and as can be seen in Fig. 6, the corresponding weight losses were 38%, 25%, 15% and 17% respectively.

Furthermore, Fig. 7 also shows that the addition of finer fibers with 20 μm diameter into the concrete caused the reduction of the optimum fiber length for spalling protection, compared to that of coarser fibers with 40 μm diameter. As can be seen in Fig. 6, for the optimum fiber length of the concrete with 10 mm aggregate, the weight loss of the concrete with the fine fibers (20 μm diameter) was 14%, whereas that of the concrete with the coarse fibers (40 μm diameter) was 25% thus showing 11% difference. Further to this result in Fig. 6, the results of the concrete containing finer fibers with other lengths were also better than that of the concrete containing coarser fibers. These results provide evidence that N is the critical parameter for predicting the performance of spalling protection as characterized in detail elsewhere by the authors [29], rather than the fiber content expressed by volume or by weight as commonly used in the open literature. Hence, in this paper, N is used to identify the optimum fiber length latter in Section 5.

4.4. Residual compressive strength after fire

Fig. 8 shows the residual compressive strengths of the concretes after fire. For the coarse fibers, for the concretes with 32 mm aggregate, the highest retained strength of 25% was obtained for the optimum fiber length of 40 mm; for the concretes with 20 mm aggregate, the highest retained strength of 23% was obtained for the optimum fiber length of 30 mm; and for the concretes with 10 mm aggregate, the highest retained strength of 7% was obtained for the optimum fiber length of 19 mm. For the fine fibers representatively added to the concrete with 10 mm aggregate, the highest retained strength of 28% was also obtained for the optimum fiber length of 12 mm. Hence, these results provide further evidence that the addition of the optimum fiber length significantly improves the fire resistance performance of concrete for a given aggregate size.

However, it was also noted that the use of small sized aggregate mixed in concrete deteriorated the residual compressive strength of the concrete: all concretes with 4 mm aggregate lost all strength after fire regardless of fiber length.

5. Identification of the optimum fiber length

For estimating the optimum fiber length in a convenient way, it is assumed that aggregates are spherical and fibers are not bending or tangling, which might vary the factor N_{crit} (Eq. (10)) to be discussed in this section.

5.1. Aggregate size factor

Introducing fibers into concrete has a number of probabilities to connect adjacent coarse aggregates in a way that they are intersected by the range from the shortest to the longest distances. Fig. 9 illustrates a schematic image of two adjacent aggregates in the concrete. It can be seen that the size of the aggregate is a contributing factor to determine the option from the range, in addition to affecting inter-aggregate spacing ℓ. To reflect the influence of the aggregate size into the proposed length of fibers, a representative parameter, mean size of the coarse aggregates used in the present concrete, is considered. This is given by:

$$d = \frac{6}{S_{tm\rho s}} \tag{9}$$

where d is the mean size of the coarse aggregates.

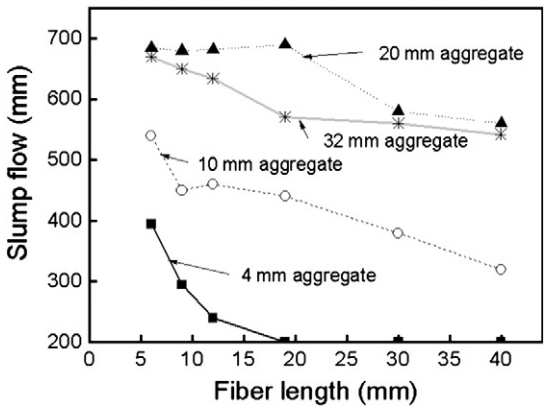

Fig. 1. Slump flow.

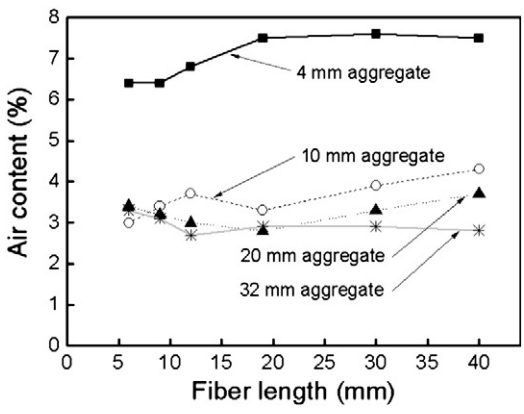

Fig. 2. Air content.

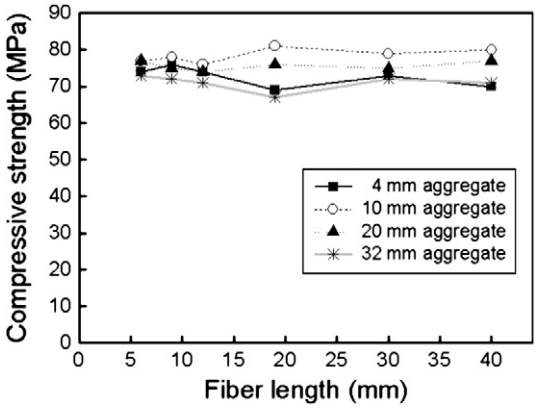

Fig. 3. Compressive strength.

5.2. Optimum fiber length

For a given fiber content, this study has confirmed that the optimum length of fibers exists as equally observed elsewhere [22,24]. The optimum fiber length can be determined based on quantitative information, such as the length of fibers, L_f and the total number of fibers per unit volume, N and inter-aggregate spacing, $\acute{\imath}$. The $\acute{\imath}$ can be simply calculated based on the C_{shell} model previously discussed in this paper, but the dimensional fiber parameters, L_f and N, need further discussion. There are two issues, which have to be defined before determining the optimum fiber length: the least fiber length and the least fiber number for the concrete to be percolated.

For the least length of fibers, it is important to consider the possibility for the percolated concrete. Hence, there is no doubt that the least fiber length should be longer than the $\acute{\imath}$, but there is maximum limit of the L_f. due to a correlation with N (Eq. (1)). For the maximum limit of the L_f, the least fiber length should be short enough to contain sufficient N to percolate the concrete for a given fiber content, so that the least length of fiber has to be in this range: $\acute{\imath}$<the least fiber length<limited maximum fiber length. To estimate the optimum fiber length in the latter

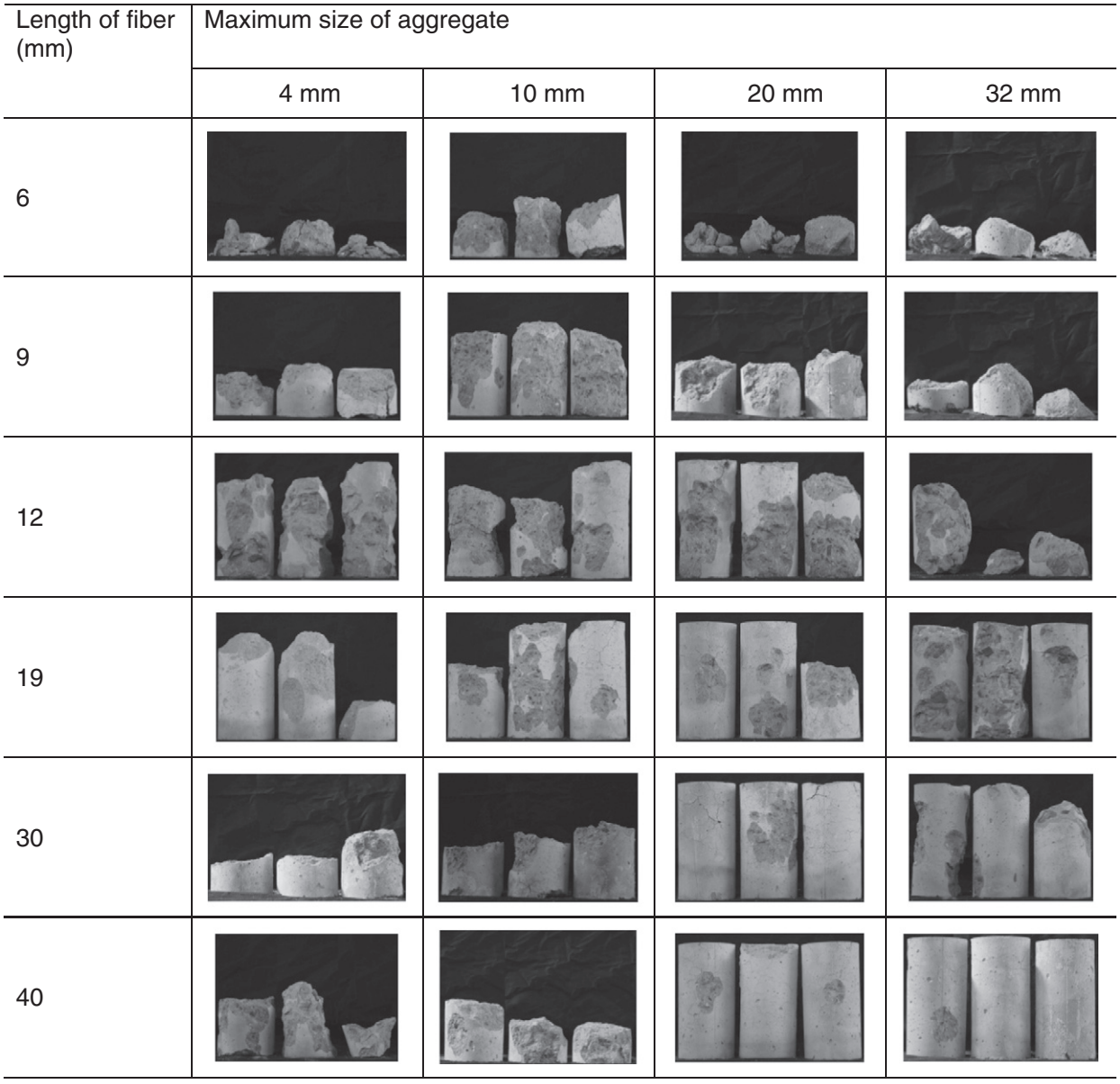

Fig. 4. Spalling extent, fiber diameter = 40 μm.

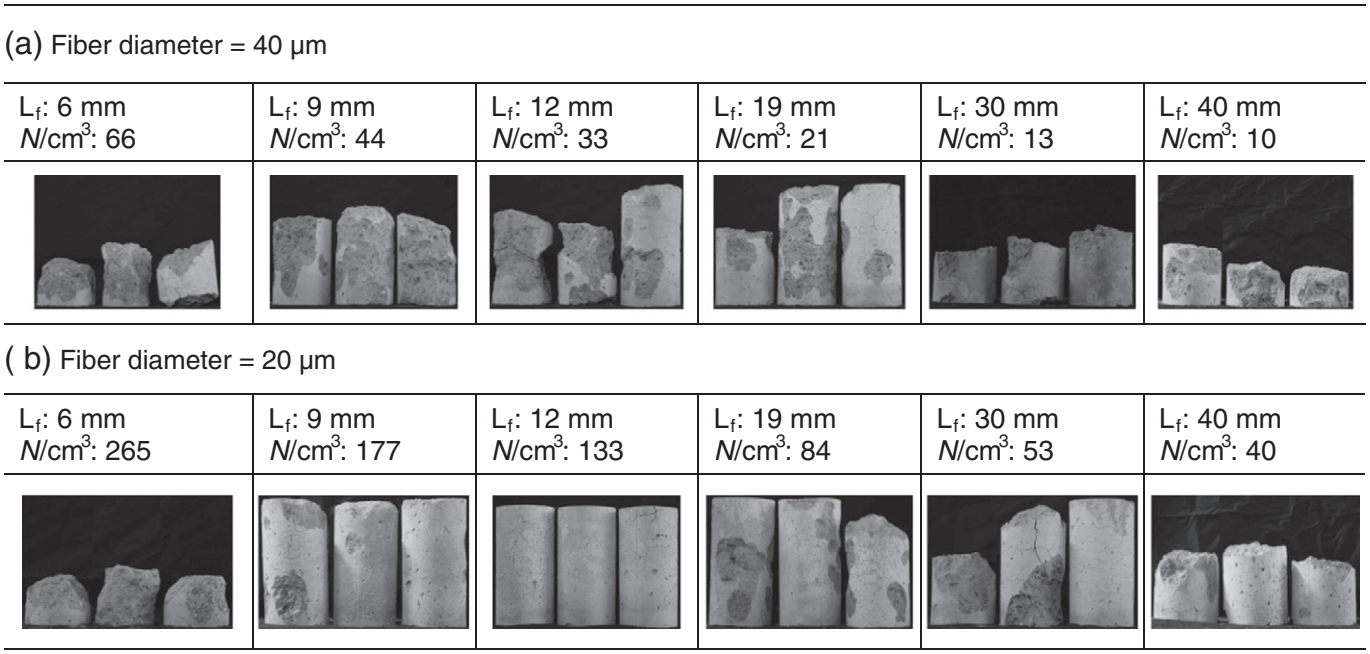

Fig. 5. Spalling extent of the concretes for the addition of fibers with equal length but different fiber number per unit volume, maximum aggregate size = 10 mm.

stage, this study introduces the least fiber length factor to be equal to the common described tangent length of adjacent spherical aggregates (Fig. 9), which is always longer than an inscribed tangent length, thus having relatively high probability to connect the adjacent aggregates.

For the least number of fibers per unit volume required for evacuating water vapor, Fig. 10 illustrates the conceptual images. In this figure, fibers are ideally distributed with black, the mean sized coarse aggregates represented by uniform spherical cores are randomly distributed with dark grey, and mortar fills the rest of pores with light grey. For the concrete just to be percolated, a number of fibers distributed in Fig. 10a are probably too many. A few fibers in Fig. 10b would be enough in theory. However, there are little chances that the fibers would be distributed in a similar way as shown in Fig. 10b. Hence, the critical number of fibers required for the percolation would be in between the number illustrated in Fig. 10a and b.

It is assumed that, for a given volume of concrete to be percolated, there is a critical threshold of the fiber number, where the least fiber length and the optimum fiber length are equal. By taking this account, the optimum length of fibers is determined as follows:

$$\zeta = (i+d)\left(\frac{N_c}{N}\right)^{\frac{1}{3}} \tag{10}$$

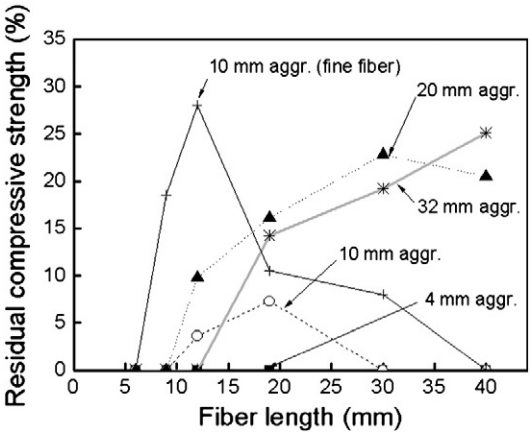

Fig. 8. Residual compressive strength.

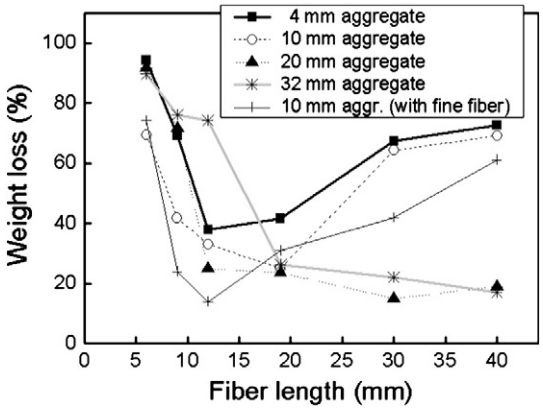

Fig. 6. Weight loss.

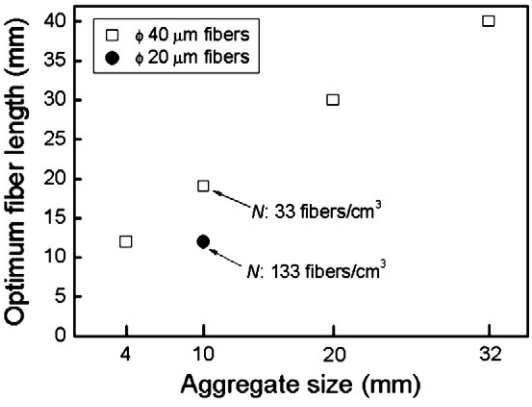

Fig. 7. The optimum fiber length as a function of aggregate size.

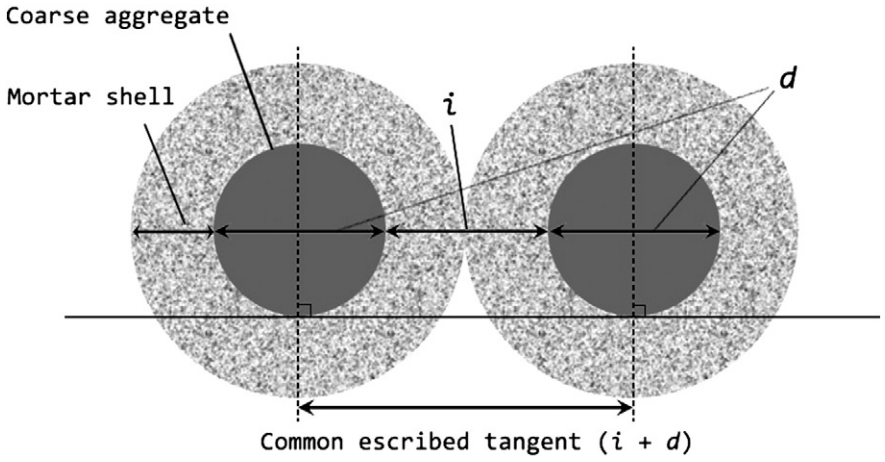

Fig. 9. Schematic illustration of two adjacent aggregates.

where ζ is the optimum length of fibers, N_c is the critical fiber number, empirically determined to be 250, which is believed to be the critical boundary (Fig. 11) of a dominant factor for fiber effectiveness parameters between L_f and N, which can be said that if N is started to be higher than N_c, the dominant factor of the fiber parameters for spalling protection is likely to be N, so that the optimum fiber length decreases to achieve increased N; and if N is lower than N_c, the dominant factor is likely to be L_f, so that the optimum fiber length increases. This is because the both parameters, L_f and N, have an effect to compensate each other in terms of the pressure relief of vapor in concrete in fire. This can be evident by evaluating N_c of each mix as shown in Table 6. The calculated optimum length, ζ, of the concrete with nylon fibers is 8.5 mm, and that of the concrete with polyvinyl alcohol fibers is 11.3 mm; but their corresponding N_c are very similar, 248 and 247 respectively. This is because smaller L_f of nylon is compensated by the higher N (491 fibers/cm^3 for 0.05% by volume of fiber content), compared to longer L_f and lower N (207 fibers/cm^3 for 0.05% by volume of fiber content) of polyvinyl alcohol. Further, Fig. 12 compares the calculated ζ and observed optimum fiber lengths from experiment, and it can be seen that they are in good agreement.

The proposed model in this study is developed based on the experimental results of the small sized concrete specimens of 100 mm diameter and 200 mm in height. It is possible that the size of specimens has an effect on thermal spalling of concrete because the capacity of larger structures store more energy [30], and the boundary conditions in relation to heat and stress of large structures are different from small specimens [31]. However, specimen size effect has been studied by some researchers [32] by testing columns with sizes ranging from 300×300 mm to 900×900 mm. They [32] did not find any size effect in specimens with fiber addition but found that there are some specimen size effects in specimens without any fiber addition. Further, they [32] also found that with larger aggregates, longer fibers were needed, which is consistent with the findings of this test series with small size specimens. The specimen size effect is an area that requires further exploration.

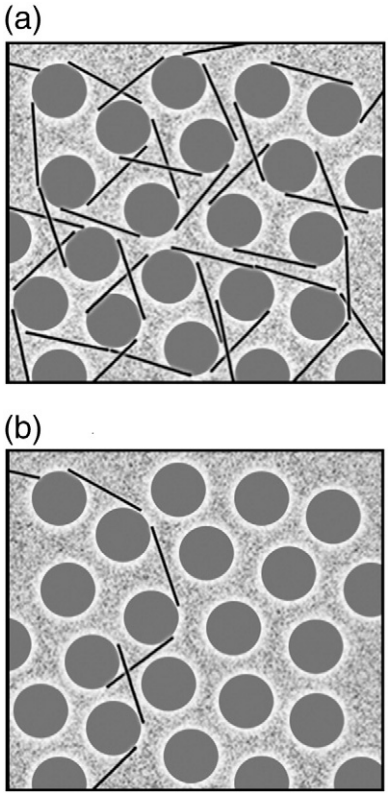

Fig. 10. Required number of fibers for percolated concrete.

6. Conclusions

In this study, the inter-aggregate spacing of coarse aggregates has been found to be an essential parameter to calculate the optimum fiber length which has been proposed for the spalling protection of any concrete of a given coarse aggregate size. The main conclusions drawn from this study are as follows:

1. The optimum length of fibers for the spalling protection of concrete is determined by three critical parameters, inter-aggregate spacing, aggregate size and critical fiber number. According to this proposed equation for the optimum fiber length, a critical threshold of the dominant fiber parameter (fiber number or fiber length) can also be estimated.

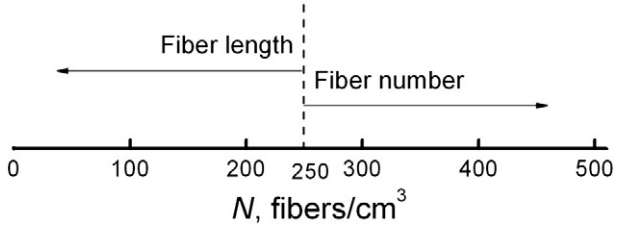

Fig. 11. Critical threshold of fiber number to determine a dominant factor of fiber parameters, from Eq. (10).

Table 6
Calculated optimum fiber length, ζ and required parameters, $N_c = 250$.

Fiber type	Fiber diameter, mm	Maximum aggr. size, mm	d (Eq. (9)), mm	$\acute{\iota}$ (Table 5)	N (Eq. (1)), cm^{-3} [b]	Critical number of fibers for each mix, cm^{-3}	ζ (Eq. (10)), mm
Polypropylene	0.040	10	5.6	2.65	21	252	20.6
Polypropylene	0.040	20	7.6	3.72	13	243	28.3
Polypropylene	0.040	32	11.1	5.42	10	142	41.3
Polypropylene	0.020	10	5.6	2.7	133	401	10.3
Nylon[a]	0.012	20	7.6	3.72	491	248	8.5
Polyvinyl alcohol[a]	0.016	20	7.6	3.72	207	247	11.3

[a] Data from [24].
[b] For fiber content: 0.05% by volume.

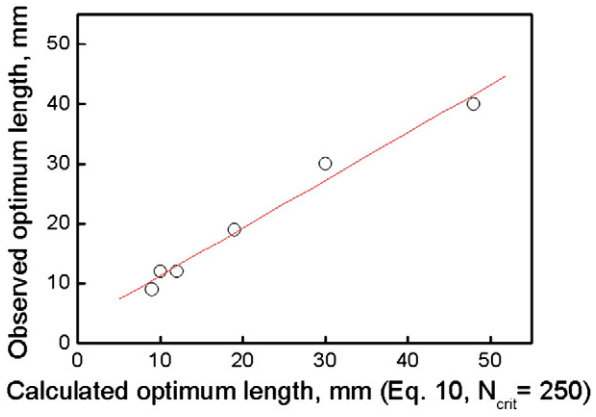

Fig. 12. Comparison of calculated and observed optimum fiber lengths.

2. The larger the size of the coarse aggregate, the longer is the optimum length of fibers for spalling protection of concrete. This is due to the fact that increasing the size of the aggregate increases the inter-aggregate spacing, thus requiring long fibers for the concretes to be percolated.
3. For a given fiber content, if the fiber diameter is decreased, the optimum fiber length decreases as well. This is because the fiber number dramatically increases and thus overtakes the effect of fiber length on the spalling protection.
4. The proposed model for calculating the optimum fiber length is based on tests on small size specimens. Further research is needed on specimen size effect to confirm this model for large structures.

Acknowledgements

The work presented in this paper was funded by the Monash Graduate Scholarship (MGS) from Monash University and Australian Research Council Grant DP 0664309.

References

[1] J.G. Sanjayan, L.J. Stocks, Spalling of high-strength silica fume concrete in fire, ACI Mater. J. 90 (1993) 170–173.
[2] C.G. Han, Concrete with spalling resistance, Mag. Korea Concr. Inst. 10 (1998) 5–10.
[3] K.D. Hertz, Limits of spalling of fire-exposed concrete, Fire Saf. J. 38 (2003) 103–116.
[4] M. Guerrieri, J. Sanjayan, F. Collins, Effect of slag on the performance of concretes in hydrocarbon fire. ACI SP225-02: Designing Concrete Structure for Fire Safety, ACI-TMS Committee 216, Fire Resist. Fire Prot. Struct. 255 (2008) 23–46.
[5] Y. Msaad, G. Bonnet, Analysis of heated concrete spalling due to restrained thermal dilation: application to the Chunnel fire, J. Eng. Mech. 132 (2006) 1124–1132.
[6] G.R. Consolazio, M.C. McVay, J.W. Rish III, Measurement and prediction of pore pressures in saturated cement mortar subjected to radiant heating, ACI Mater. J. 95 (1998) 525–536.
[7] L.T. Phan, N.J. Carino, Effects of test conditions and mixture proportions on behavior of high-strength concrete exposed to high temperature, ACI Mater. J. 99 (2002) 54–66.
[8] P. Kalifa, G. Chene, C. Galle, High-temperature behaviour of HPC with polypropylene fibers from spalling to microstructure, Cem. Concr. Res. 31 (2001) 1487–1499.
[9] D. Gawin, F. Pesavento, B.A. Schrefler, Towards prediction of the thermal spalling risk through a multi-phase porous media model of concrete, Comput. Meth. Appl. Mech. Eng. 195 (2006) 5707–5729.
[10] J.C. Mindequia, P. Pimienta, A. Noumowé, M. Kanema, Temperature, pore pressure and mass variation of concrete subjected to high temperature – experimental and numerical discussion on spalling risk, Cem. Concr. Res. 40 (2010) 477–487.
[11] D.P. Bentz, Fibers, percolation, and spalling of high-performance concrete, ACI Mater. J. 97 (2000) 351–359.
[12] D. Stauffer, A. Aharony, Introduction to percolation theory, 2nd ed. Taylor and Francis, London, 1992.
[13] K.L. Scrivener, K.M. Nemati, The percolation of pore space in the cement paste/aggregate interfacial zone of concrete, Cem. Concr. Res. 26 (1996) 35–40.
[14] J.J. Zheng, C.Q. Li, X.Z. Zhou, Thickness of interfacial transition zone and cement content profiles around aggregates, Mag. Conc. Res. 7 (2005) 397–406.
[15] K.L. Scrivener, Backscattered electron imaging of cementitious microstructures: understanding and quantification, Cem. Concr. Res. 26 (2004) 935–945.
[16] Z. Bayasi, M.A. Dhaheri, Effect of exposure to elevated temperature on polypropylene fiber-reinforced concrete, ACI Mater. J. 99 (2002) 22–26.
[17] A. Bilodeau, V.K.R. Kodur, G.C. Hoff, Optimization of the type and amount of polypropylene fibers for preventing the spalling of lightweight concrete subjected to hydrocarbon fire, Cem. Concr. Res. 26 (2004) 163–174.
[18] C.G. Han, M.C. Han, Y.S. Heo, Improvement of residual compressive strength and spalling resistance of high-strength RC columns subjected to fire, Constr. Build. Mater. 23 (2009) 107–116.
[19] Y.S. Heo, J.G. Sanjayan, C.G. Han, M.C. Han, Construction application of Fibre/Mesh method for protecting concrete columns in fire, Constr. Build. Mater. 25 (2011) 2928–2938.
[20] S.L. Suhaendi, T. Horiguchi, Effect of short fibers on residual permeability and mechanical properties of hybrid fiber reinforced high strength concrete after heat exposition, Cem. Concr. Res. 36 (2006) 1672–1678.
[21] E.J. Garboczi, K.A. Snyder, J.F. Douglas, M.F. Thorpe, Geometrical percolation threshold of overlapping ellipsoids, Phys. Rev. E 52 (1995) 819–828.
[22] Y.S. Heo Influential factors on fire resistance performance of ultra high strength concrete and mechanism models of spalling phenomenon. Master thesis, Cheongju University Korea (2006).
[23] Y.S. Heo, J.G. Sanjayan, C.G. Han, M.C. Han, Synergistic effect of combined fibers for spalling protection of concrete in fire, Cem. Concr. Res. 40 (2010) 1547–1554.
[24] Y.S. Heo, J.G. Sanjayan, C.G. Han, M.C. Han, Critical parameters of nylon and other fibres for spalling protection of high strength concrete in fire, Mater. Struct. 44 (2011) 599–610.
[25] R.P. Chapuis, P.P. Légaré, A simple method for determining the surface area of fine aggregate and fillers on asphalt mixture, In effects of aggregates and mineral fillers on asphalt mixture performance, American Society for Testing and Materials, ASTM STP 1147, , 1992, pp. 177–186.
[26] A.G. Loudon, The computation of permeability from simple soil test, Geotechnique 3 (1952) 165–183.
[27] P.R. Rangaraju, J. Olek, S. Diamond, An investigation into the influence of inter-aggregate spacing and the extent of the ITZ on properties of Portland cement concretes, Cem. Concr. Res. 40 (2010) 1601–1608.
[28] N. Neithalath, M.S. Sumanasooriya, O. Deo, Characterizing pore volume, sizes, and connectivity in previous concretes for permeability prediction, Mater. Charact. 61 (2010) 802–813.
[29] Y.S. Heo, J.G. Sanjayan, C.G. Han, M.C. Han, Limited effect of diameter of fibres on spalling protection of concrete in fire, Mater. Struct. (2011), doi:10.1617/s11527-011-9768-z.
[30] V.K.R. Kodur, L. Phan, Critical factors governing the fire performance of high strength concrete system, Fire Saf. J. 42 (2007) 482–488.
[31] R. Jansson, L. Boström, Spalling of concrete exposed to fire. Fire technology SP report, SP Technical Research Institute of Sweden, 2008.
[32] H.K. Jung, H.J. Son, B.H. Lee, M.C. Han, S.H. Yang, C.G. Han, Spalling of high strength concrete depending on specimen sizes, Proc.Archit. Inst. Korea 29 (2009) 571–574.